

# Superhalogen and Superacid.

## Superalkali and Superbase

*Andrey V. Kulsha<sup>†‡\*</sup>, Dmitry I. Sharapa<sup>ψ‡\*</sup>*

<sup>†</sup> Lyceum of Belarusian State University, 8 Ulijanauskaja str., Minsk 220030, Belarus

<sup>ψ</sup> Chair of Theoretical Chemistry and Interdisciplinary Center for Molecular Materials, Friedrich-Alexander-Universität Erlangen-Nürnberg, Egerlandstraße3, 91058 Erlangen, Germany

KEYWORDS: Superhalogen, superacid, superalkali, superbase, DLPNO-CCSD(T)

ABSTRACT A superhalogen  $F@C_{20}(CN)_{20}$  and a superalkali  $NC_{30}H_{36}$  together with corresponding Brønsted superacid and superbase were designed and investigated on DFT and DLPNO-CCSD(T) levels of theory. Calculated compounds have outstanding properties (electron affinity, ionization energy, pKa and proton affinity respectively). We consider superacid  $H[F@C_{20}(CN)_{20}]$  to be able to protonate molecular nitrogen, while  $NC_{30}H_{35}$  superbase should easily deprotonate  $SiH_4$ . Neutral  $NC_{30}H_{36}$  should form a metallic metamaterial with extreme properties like remarkable transparency to visible light due to infrared plasmonic wavelength. Yet stronger superbases with predicted proton affinity of more than 15 eV were designed. The stability of these structures is discussed, while some of the previous predictions concerning Brønsted superacids and superbases of record strength are doubted.

## 1. Introduction

Traditionally, a superhalogen is a molecule with high electron affinity, which forms a stable anion. A good example is  $\text{AuF}_6$  with electron affinity of about 8.2 eV.<sup>1</sup> Just in the same way a superalkali is a molecule with low ionization energy, which forms a stable cation. A common example is  $\text{Li}_3\text{O}$  with ionization energy of 3.6 eV.<sup>2</sup> Superhalogen anions usually have low proton affinities leading to superacids, while superalkali cations usually have high deprotonation energies leading to superbases.<sup>3,4</sup>

However, few of the known superhalogen and superalkali neutral molecules are stable in condensed phase.<sup>5-7</sup> The goal of this article was to design structures that could behave close to real alkali and halogen atoms, but with extreme properties.

## 2. Superhalogen and Superacid

### 2.1. Design.

The idea of symmetric cage surrounded with electron-withdrawing groups is barely new. For example, one of the strongest currently known Brønsted acids is fluorocarborane acid  $\text{H}[\text{CHB}_{10}\text{F}_{11}]$ .<sup>8</sup> Its anion is formed by a carborane cage surrounded with fluorine atoms and shows superhalogenic behavior. A similar structure with cyano groups,  $\text{B}_{12}(\text{CN})_{12}^{2-}$ , was suggested as a highly stable dianion with second electron bound by 5.3 eV.<sup>9</sup>

Going this way, we designed a dodecahedrane cage with 20 cyano groups. Some quick DFT estimations suggested that this structure should be much more stable than halogenated

dodecahedranes like  $C_{20}F_{20}$  or  $C_{20}Cl_{20}$  because of a large noble-gas-like HOMO-LUMO gap. Therefore, the last step to superhalogen was the encapsulation of a single fluorine atom. It is known that atomic fluorine has lower electron affinity than atomic chlorine because of large density of negative charge in fluoride anion due to its small radius. Encapsulation into  $C_{20}(CN)_{20}$  helps to delocalize the excess of negative charge over twenty electron-withdrawing groups and makes  $F@C_{20}(CN)_{20}^-$  a very stable anion (Figure 1). Hereinafter we abbreviate  $F@C_{20}(CN)_{19}$  structure as **X**, so the short notation for the superhalogenic anion is  $NCX^-$ .

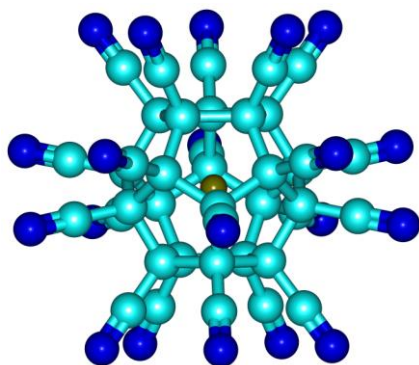


**Figure 1.** Structure of  $F@C_{20}(CN)_{20}$ . Color coding: C – cyan, N – dark blue, F – olive.

## 2.2. Computational details.

Recently developed DLPNO approach to coupled cluster theory<sup>10-15</sup> induced us to use this level of theory for the single-point computations as implemented in ORCA 4.0 package.<sup>16</sup> This method was shown to provide results of canonical coupled-cluster quality.<sup>17-23</sup> All the calculations were performed for gas phase.

The standard cc-pVTZ basis set<sup>24</sup> was chosen for all atoms except for nitrogen, where maug-cc-pVTZ<sup>25</sup> was used because nitrogen atoms fill the surface of the anion. The corresponding auxiliary

basis sets were cc-pVTZ/C and aug-cc-pVTZ/C,<sup>26</sup> respectively. Test calculations (Table 1) were performed with 6-311G\* basis set.<sup>27</sup>

For geometry optimizations and zero-point energy estimations we chose a DFT functional PBE0<sup>28</sup> as implemented in Gaussian16 package<sup>29</sup>. This functional is known to produce overall good geometries for organic structures. Usually it underestimates C≡N bond lengths nearly by 0.01Å, and this is the most energy-sensitive deviation for our systems, but the corresponding shift of energy differences appeared to be negligible for our purposes (about 0.002 eV). PBE0 zero-point energies were not scaled.

Most of the structures accounted are closed-shell singlets with HOMO-LUMO gap sufficiently large to use NormalPNO cutoffs in ORCA. However, neutral NCX is a doublet with quite small HOMO-LUMO gap; hence we used UHF wavefunction with TightPNO cutoffs for electron affinity determination.<sup>18, 19, 30</sup> That choice is confirmed with results of test computations collected in Table 1.

**Table 1.** Test calculations. Proton affinity of NCX<sup>-</sup> and electron affinity of NCX.

NormalPNO vs. TightPNO approximations. PBE0 geometry, no ZPE corrections.

Method	PA(NCX <sup>-</sup> ) / eV RHF, 6-311G*	EA(NCX) / eV UHF, 6-311G*
Canonic CCSD <sup>a</sup>	9.438	11.131
DLPNO-CCSD / NormalPNO	9.433	10.909
DLPNO-CCSD / TightPNO	9.438	11.157
DLPNO-CCSD(T) / NormalPNO	9.436	10.538
DLPNO-CCSD(T) / TightPNO	9.444	10.649

<sup>a</sup> performed in Gaussian16.

### 2.3. Electron affinity.

The ground state of NCX<sup>-</sup> anion is a closed-shell singlet of  $I_h$  symmetry. According to PBE0 functional, cage C—C bond lengths are 1.586Å, so the distance from the center fluorine to cage carbon is 2.222Å. Outer C—C bond lengths are shortened to 1.460Å, while C≡N bond lengths are 1.148Å.

Neutral NCX radical has an open-shell doublet ground state with lower symmetry  $D_{3d}$  due to Jahn-Teller effect. However, the stretch along  $C_3$  axis is quite small (only +0.008Å between axial atoms of the cage), so it may be smoothed by zero-point vibrations. Table 2 shows the results of electron affinity calculations performed.

**Table 2.** Electron affinity of NCX.

Source	EA(NCX) / eV
PBE0	9.766
PBE0 ZPE correction	-0.161
DLPNO-CCSD	11.428
DLPNO-CCSD(T)	10.913
DLPNO-CCSD(T) + ZPE	<b>10.752</b>

ZPE scaling, basis set enrichment and quadruplets accounting should probably push the final value a bit higher, so we round our result to 10.8 eV. That makes NCX, to our knowledge, a superhalogen with the highest electron affinity ever predicted. However, higher affinities should be possible, and an example will be shown later in section 2.7.

## 2.4. Superacid.

The most favorable protonation site in  $\text{NCX}^-$  is nitrogen atom. The resulting molecule  $\text{HNCX}$  has singlet ground state of  $C_{3v}$  symmetry with dipole moment of 13.96 Debye and NH bond length of 1.008 Å according to PBE0 functional. Gas phase proton affinity of  $\text{NCX}^-$  was estimated as 9.3 eV (Table 3).

**Table 3.** Proton affinity of  $\text{NCX}^-$ .

Source	PA( $\text{NCX}^-$ ) / eV
PBE0	9.681
PBE0 ZPE correction	-0.276
DLPNO-CCSD	9.586
DLPNO-CCSD(T)	9.579
DLPNO-CCSD(T) + ZPE	<b>9.303</b>

$\text{HNCX}$  superacid also features the strongest single bond known. Indeed, the dissociation energy  $\text{HNCX} = \text{H} + \text{NCX}$  could be estimated as  $\text{PA}(\text{NCX}^-) + \text{EA}(\text{NCX}) - \text{IE}(\text{H}) = 9.3 \text{ eV} + 10.8 \text{ eV} - 13.6 \text{ eV} = 6.5 \text{ eV}$ , or about 150 kcal/mol.

We decided to compare the acidity of  $\text{HNCX}$  with the acidity of fluorocarborane superacid  $\text{H}[\text{CHB}_{11}\text{F}_{11}]$  which is able to protonate  $\text{CO}_2$ .<sup>31</sup> It is known that in highly acidic media proton tends to form bridged structures,<sup>32</sup> so we compared both HA and  $\text{AHA}^-$  for  $\text{A} = \text{CHB}_{11}\text{F}_{11}$  and  $\text{A} = \text{NCX}$ .

The most favorable protonation site in  $\text{CHB}_{11}\text{F}_{11}$  appeared to be fluorine atom most distant from carbon, leading to  $C_s$  symmetry for neutral  $\text{H}[\text{CHB}_{11}\text{F}_{11}]$  and  $C_{2h}$  symmetry for  $\text{H}[\text{CHB}_{11}\text{F}_{11}]_2^-$  anion (Figure 2), while  $\text{H}[\text{NCX}]_2^-$  anion features  $D_{3d}$  symmetry. Both bridged anions contain short

symmetrical hydrogen bonds with  $N\cdots H$  distances of 1.259 Å in  $H[NCX]_2^-$  and  $F\cdots H$  distances of 1.138 Å in  $H[CHB_{11}F_{11}]_2^-$ .

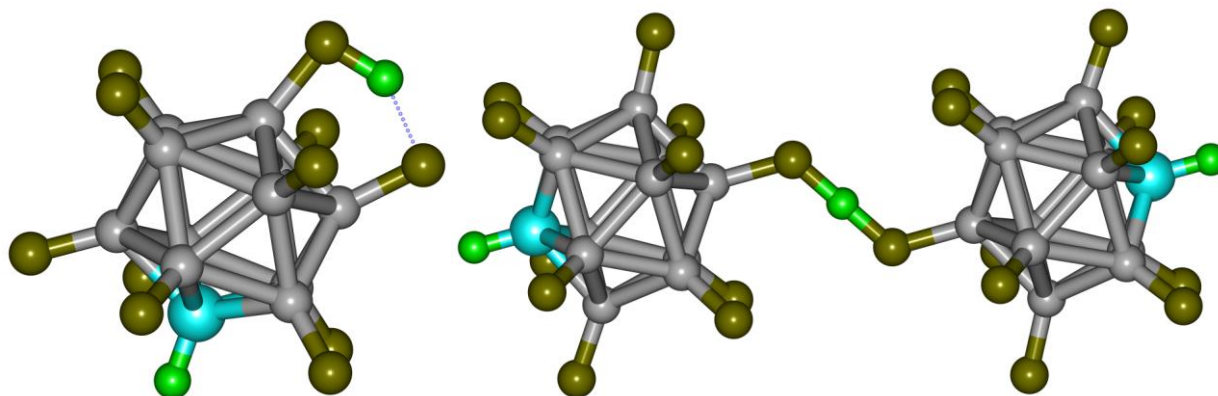


**Figure 2.**  $H[CHB_{11}F_{11}]$  (left) and  $H[CHB_{11}F_{11}]_2^-$  anion (right). Color coding: C – cyan, B – silver, F – olive, H – green.

**Table 4.** Theoretical acidity comparison of  $HNCX$  and  $H[CHB_{11}F_{11}]$ .

DLPNO-CCSD(T) + PBE0 ZPE correction (eV).

Proton binding way	A = NCX	A = $CHB_{11}F_{11}$ <sup>a</sup>
$H^+ + A^- = HA$	-9.303	-9.812
$H^+ + 2A^- = AHA^-$	-10.690	-11.425

<sup>a</sup> maug-cc-pVTZ basis set was used for fluorine atoms.

According to results shown in Table 4,  $HNCX$  should be much stronger acid than  $H[CHB_{11}F_{11}]$ , so we wondered the capability of  $HNCX$  to protonate molecular nitrogen and to produce a bridged cation  $[NNHNN]^+$  first observed in 1999.<sup>33</sup>

We considered the ion pair  $[NNHNN]^+[NCX]^-$  and compared it to similar ion pairs formed by 1,2-dicyanocyclopentadiene and pentacyanotoluene in acetonitrile solution. For  $[NNHNN]^+[NCX]^-$

we found the ground minimum geometry of  $C_s$  symmetry with almost linear NNHNN trapped between three nearby CN needles.  $[(CH_3CN)_2H]^+[C_5H_3(CN)_2]^-$  appeared to have  $C_{2v}$  symmetry with symmetrical cation embowed around two cyano groups of anion, while in  $[(CH_3CN)_2H]^+[CH_2C_6(CN)_5]^-$  methyl groups of cation snuggle to cyano groups in *ortho*- and *para*-positions of benzene ring (Figure 3).

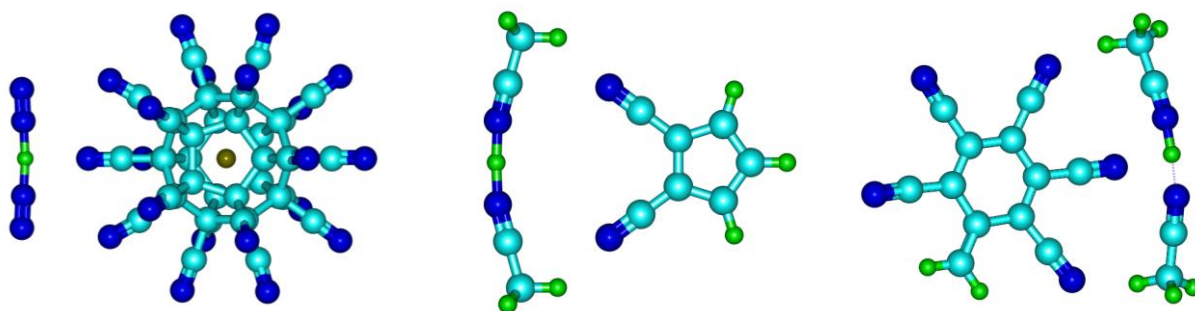


**Figure 3.**  $[NNHNN]^+[NCX]^-$  (left),  $[(CH_3CN)_2H]^+[C_5H_3(CN)_2]^-$  (middle),  $[(CH_3CN)_2H]^+[CH_2C_6(CN)_5]^-$  (right). Color coding: C – cyan, N – dark blue, H – green, F – olive.

**Table 5.** Proton solvation comparison in acetonitrile and nitrogen.

DLPNO-CCSD(T) + PBE0 ZPE correction.

Gas phase reaction	Energy / eV
$HNCX + 2N_2 = [NNHNN]^+[NCX]^-$	0.975
$H[C_5H_3(CN)_2] + 2CH_3CN = [(CH_3CN)_2H]^+[C_5H_3(CN)_2]^-$	0.879
$H[CH_2C_6(CN)_5] + 2CH_3CN = [(CH_3CN)_2H]^+[CH_2C_6(CN)_5]^-$	1.305

Experimental pKa values in CH<sub>3</sub>CN are 10.17 for 1,2-dicyanocyclopentadiene<sup>34</sup> and 20.14 for pentacyanotoluene<sup>35</sup>; so simple linear interpolation gives us pKa = 12.4 in nitrogen for HNCX. However, that very rough result should be treated only as qualitative estimation providing some evidence to tiny but nonzero chance that molecular nitrogen could be indeed protonated by our superacid.

The possibility of auto-ionization of HNCX was also considered. Neutral acid has five possible protonation sites to form HNCXH<sup>+</sup> tautomers. Their energy depends on the distance between protons (the larger is distance, the lower is energy), so the most favorable tautomer has *D*<sub>3d</sub> symmetry. That fact suggests that in condensed phase HNCX will probably form a linear polymer •••H•••[NCX]•••H•••[NCX]••• instead of cyclic or zigzag-shaped clusters typical for HF. The proton affinity of neutral HNCX was estimated as 7.4 eV; accounting earlier results, the enthalpy of autoionization process 3HNCX = H[NCX]<sub>2</sub><sup>-</sup> + HNCXH<sup>+</sup> appeared to be as small as +0.5 eV in gas phase (Table 6).

**Table 6.** Autoionization energy for HNCX.

DLPNO-CCSD(T) + PBE0 ZPE correction.

Gas phase reaction	Energy / eV
$\text{HNCX} = \text{NCX}^- + \text{H}^+$	9.303
$\text{HNCX} + \text{H}^+ = \text{HNCXH}^+$	-7.395
$\text{HNCX} + \text{NCX}^- = \text{H}[\text{NCX}]_2^-$	-1.388
$3\text{HNCX} = \text{H}[\text{NCX}]_2^- + \text{HNCXH}^+$	<b>0.520</b>

For comparison, the enthalpy change for a similar process  $3\text{HF} = \text{HF}_2^- + \text{H}_2\text{F}^+$  is +9.2 eV in gas phase, so we expect a high degree of autoionization for HNCX.

## 2.5. Other simple derivatives.

As well as common halogen atoms, neutral NCX readily forms covalent bonds with atoms other than hydrogen and can also exist as a dimer  $[\text{NCX}]_2$ . Actual bonds are formed by nitrogen atoms of cyano groups.

The  $[\text{NCX}]_2$  molecule is analogous to halogen diatomics (Figure 4). It has singlet ground state of  $D_{3d}$  symmetry featuring NN bond of length 1.238Å which is close to double bond in  $\text{N}_2\text{H}_2$ . Another molecule, FNCX, is an analog of interhalogen diatomics. It has  $C_{3v}$  singlet ground state with dipole moment of 13.04 Debye that is almost as large as of HNCX, suggesting an outstanding electronegativity of our superhalogen. Quite short FN bond of 1.249Å shows partially double character just like FC bond in FCN.

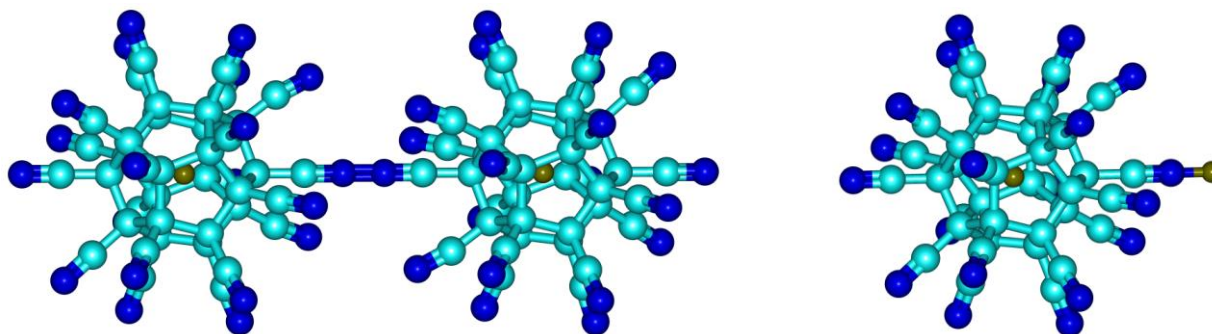


**Figure 4.**  $[\text{NCX}]_2$  (left) and FNCX (right). Color coding: C – cyan, N – dark blue, F – olive.

Direct calculation of dissociation energies (DE) for  $[\text{NCX}]_2$  and FNCX would need UHF wavefunction with TightPNO cutoffs. In order to avoid heavy calculations, we made sideway estimates using gas phase reactions between closed-shell structures (Table 7).

**Table 7.** Supplemental calculations for dissociation energy estimations.

DLPNO-CCSD(T) + PBE0 ZPE correction.

Gas phase reaction	Energy / eV
$[\text{NCX}]_2 + 2e^- = 2\text{NCX}^-$	-17.439
$[\text{NCX}]_2 + \text{HF} = \text{HNCX} + \text{FNCX}^a$	-0.097

<sup>a</sup> Negative  $\Delta H$  suggests that  $[\text{NCX}]_2$  would oxidize HF.

Thus,  $\text{DE}([\text{NCX}]_2)$  was estimated as  $2 \cdot \text{EA}(\text{NCX}) - 17.439 \text{ eV} = 4.065 \text{ eV} \approx 4.1 \text{ eV}$ , or about 94 kcal/mol, which is much higher than for diatomic halogens. Taking into account previously estimated  $\text{DE}(\text{HNCX})$  of 6.5 eV and experimental value of  $\text{DE}(\text{HF}) = 5.9 \text{ eV}$ <sup>36</sup>, we obtain  $\text{DE}(\text{FNCX}) = (4.1 + 5.9 + 0.1 - 6.5) \text{ eV} = 3.6 \text{ eV}$ , or about 83 kcal/mol.

## 2.6. Stability.

It is clear that our predictions have little sense until the stability of our superhalogen and its derivatives is examined. First, the cage C—C bond in  $\text{NCX}^-$  is predicted to be about 0.05 Å longer than C—C bond in ethane, hinting at some strain. Therefore, we wondered how much energy the encapsulation takes.

The encapsulation of fluorine atom, fluoride anion and neon atom (Table 8) was considered. Again, to avoid heavy calculations, the sideway reaction  $\text{C}_{20}(\text{CN})_{20} + \text{HF} = \text{HNCX}$  was used together with known values of  $\text{EA}(\text{F}) = 3.401 \text{ eV}$ <sup>37</sup> and  $\text{PA}(\text{F}^-) = 16.063 \text{ eV}$ <sup>36</sup>.

**Table 8.** Encapsulation energies for F<sup>-</sup>, F and Ne. DLPNO-CCSD(T) + PBE0 ZPE correction.

Gas phase reaction	Energy / eV
$C_{20}(CN)_{20} + Ne = Ne@C_{20}(CN)_{20}$	3.055
$C_{20}(CN)_{20} + HF = HNCX$	1.473
$C_{20}(CN)_{20} + F^- = NCX^-$	-5.287 <sup>a</sup>
$C_{20}(CN)_{20} + F = NCX$	2.064 <sup>b</sup>

<sup>a</sup> Calculated as 1.473 eV – PA(F<sup>-</sup>) + PA(NCX<sup>-</sup>).

<sup>b</sup> Calculated as -5.287 eV – EA(F) + EA(NCX).

Exothermic encapsulation of fluoride anion is expectative because of negative charge delocalization noted earlier. However, for isoelectronic process of neon encapsulation we have 8.3 eV larger energy, suggesting some repulsion between the noble electron cloud and the cage. Surprisingly, for fluorine atom the encapsulation is 1 eV more profitable despite its larger radius compared to neon. That could be explained with proximity of energies, and therefore significant correlation, between fluorine-localized and cage-localized molecular orbitals. In other words, the fluorine atom fits the cage in some sense.

Thus, discussed superhalogen is thermodynamically unstable against the loss of fluoride atom by about 2 eV. That is not too much to our opinion, particularly if we take into account the kinetic barrier, which should be very high because of tight pentagonal holes of the cage. A similar barrier for smaller helium atoms was proven high in 1999.<sup>38</sup>

Further calculations revealed the most vulnerable place in the superhalogen molecule. It is the outer C—C bond despite its partially double character. The key is that fluorine atom may attack one of the cage carbons from inside, pulling it inward and leaving the CN group alone, just like in

S<sub>N</sub>2. The resulting molecule **X** (structurally related to “in-adamantane”<sup>39</sup>) has a singlet ground state of C<sub>3v</sub> symmetry with C—F bond length of 1.431 Å (Figure 5). That large bond length is the result of carbon cage strain.

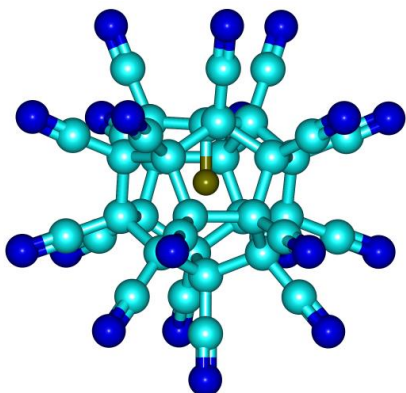


**Figure 5.** Structure of **X** molecule C<sub>20</sub>(*in-F*)(CN)<sub>19</sub>. Color coding: C – cyan, N – dark blue, F – olive.

The formation of **X** from superhalogen and its derivatives is considered in Table 9. As before, sideways calculations were performed using known values of EA(CN) = 3.862 eV and PA(CN<sup>-</sup>) = 15.199 eV<sup>40</sup>.

**Table 9.** Stability against the formation of **X**. DLPNO-CCSD(T) + PBE0 ZPE correction.

Gas phase reaction	Energy / eV
[NCX] <sub>2</sub> = NCCN + 2 <b>X</b>	-2.291
FNC <b>X</b> = FCN + <b>X</b>	-2.001
HNC <b>X</b> = HCN + <b>X</b>	0.810
NCX <sup>-</sup> = CN <sup>-</sup> + <b>X</b>	6.707 <sup>a</sup>
NC <b>X</b> = CN + <b>X</b>	-0.183 <sup>b</sup>

<sup>a</sup> Calculated as 0.810 eV + PA(CN<sup>-</sup>) – PA(NCX<sup>-</sup>).

<sup>b</sup> Calculated as  $6.707 \text{ eV} + \text{EA}(\text{CN}) - \text{EA}(\text{NCX})$ .

These results show that the superhalogen anion is very stable against the cage concaving, while the superacid is moderately stable. Possible formation of dicyanogen and cyanogen fluoride makes  $[\text{NCX}]_2$  and  $\text{FNCX}$  thermodynamically unstable, although the direct attack of the cage carbon would produce  $\text{FNC}$  and  $\text{CNNC}$  needing rearrangement. As for  $\text{NCX}$  itself, the loss of cyanide radical appeared to be a bit exothermic, but the kinetic barrier could be high enough for  $\text{NCX}$  to survive, say, at the temperature of liquid nitrogen.

On the other hand,  $\text{X}$ -type structure could be used as a precursor to  $\text{NCX}^-$ . Indeed, if the concaved cage was built around the  $\text{C—F}$  fragment, it would be possible to attach a cyanide anion from outside detaching the fluorine atom inwards.

## 2.7. Possible improvements.

The limits can always be pushed further. We compared our superhalogen to a few other structures, trying to improve either electron affinity or proton affinity value.

First of all, two larger carbon cages were considered:  $\text{C}_{24}$  of  $D_{6d}$  symmetry and  $\text{C}_{28}$  of  $T_d$  symmetry, both decorated with cyano groups (Figure 6). However, DFT estimates show that electron affinity does not grow this way (Table 10). Calculated Hartree-Fock HOMO energies for anions support this trend.

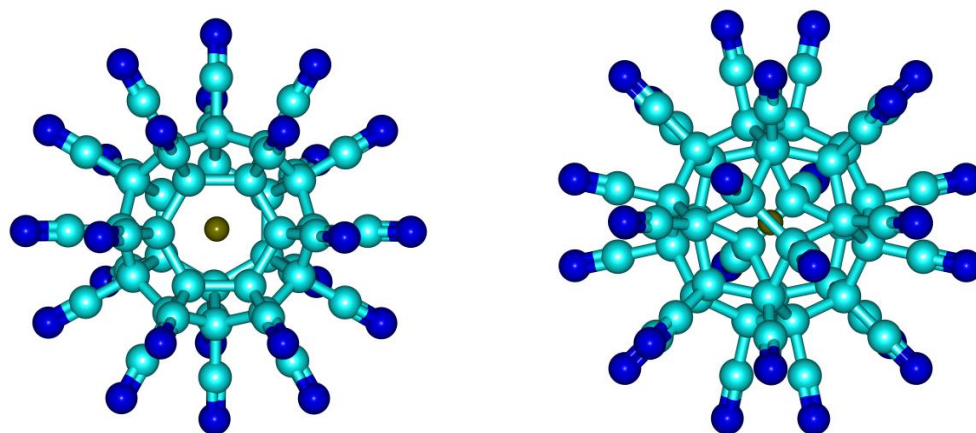


**Figure 6.**  $F@D_{6d}\text{-C}_{24}(\text{CN})_{24}$  (left) and  $F@T_d\text{-C}_{28}(\text{CN})_{28}$  (right). Color coding: C – cyan, N – dark blue, F – olive.

**Table 10.** Electron affinity comparison for different cages.

Structure	EA / eV (PBE0 without ZPE corrections)	HOMO energy / eV (HF wavefunction for anion)
$F@C_{20}(\text{CN})_{20}$	9.766	-11.768
$F@C_{24}(\text{CN})_{24}$	9.502	-11.482
$F@C_{28}(\text{CN})_{28}$	9.484	-11.455

Thus, dodecahedrane cage seems to be the best fit for fluorine atom. Another try to improve the structure was changing cyano groups to  $\text{CF}_3$  ones, but that quickly lead to overcrowding of fluorine atoms, preventing the proper delocalization of negative charge.

Looking at carborane cages, we noticed that the cage  $\text{CB}_{11}$  of  $C_{5v}$  symmetry, decorated with 12  $\text{CF}_3$  groups (Figure 7), has less crowding and was already proposed in 2000.<sup>41</sup> As well as  $\text{B}_{12}(\text{CF}_3)_{12}$  and related structures, it was suggested by Ivo Leito and coworkers<sup>42,43</sup> as an anion for a Brønsted superacid of record-breaking strength. Unfortunately, we found that claim to be wrong

since  $\text{CF}_3$  group is not stable in highly acidic media. To be precise, fluorine atom appears to be the most favorable protonation site, and once it is protonated, HF molecule is eliminated from the structure without any notable barrier. That happens because of larger electronegativity of carbon compared to hydrogen, which makes H—F single bond stronger than C—F single bond. Surprisingly, the authors were aware of that issue,<sup>44</sup> but somehow ignored it (Figure 8).

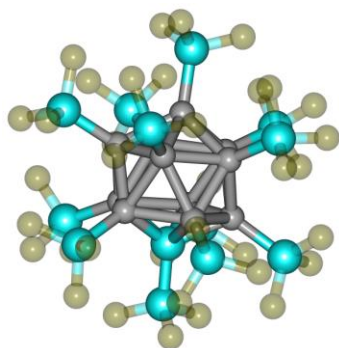


**Figure 7.**  $\text{CB}_{11}(\text{CF}_3)_{12}^-$  anion. Color coding: C – cyan, B – silver, F – transparent olive.

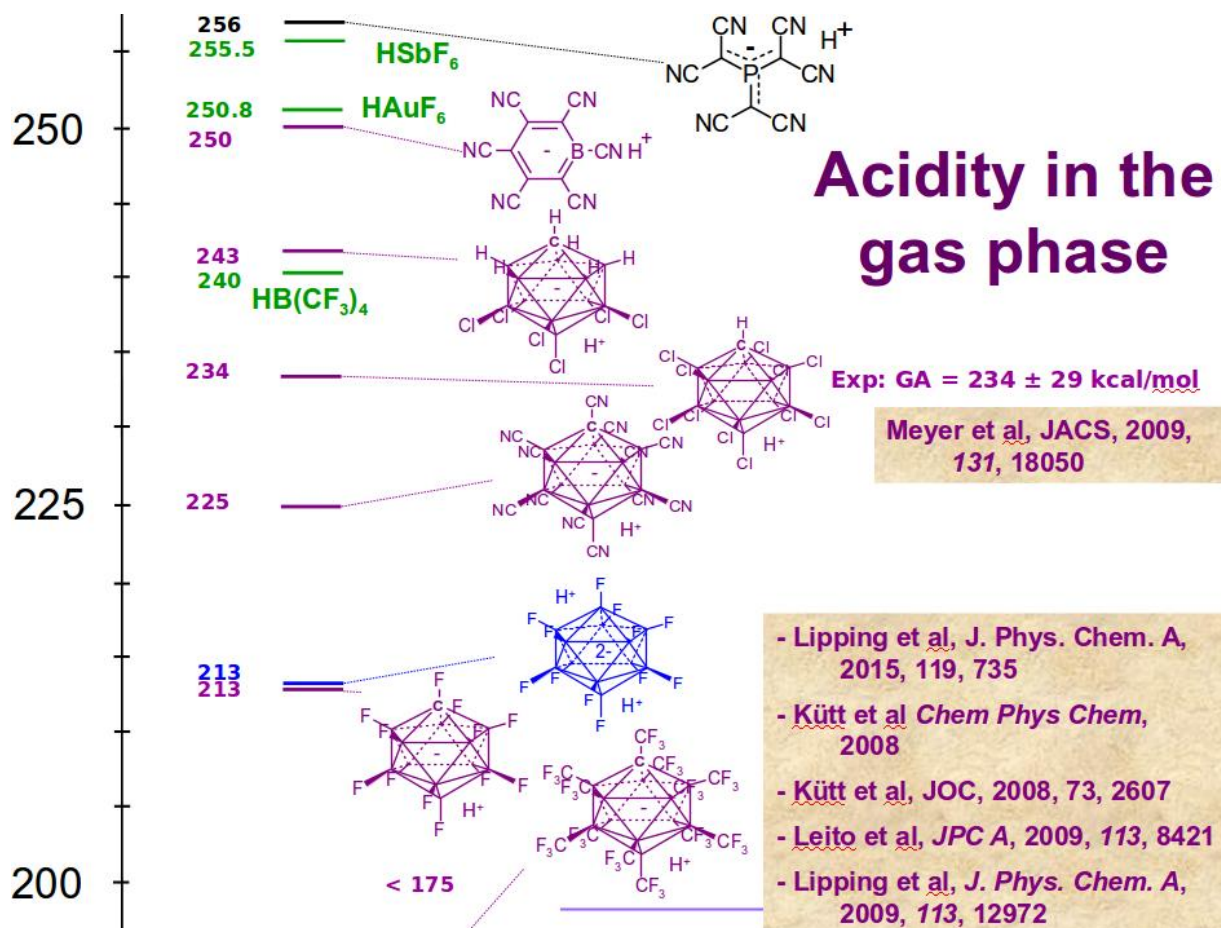


**Figure 8.** A claim of record-strength acidity of H[CB<sub>11</sub>(CF<sub>3</sub>)<sub>12</sub>]. Represented from Ref.<sup>45</sup> with permission.

As for electron affinity of CB<sub>11</sub>(CF<sub>3</sub>)<sub>12</sub>, the predicted value of 8.8 eV<sup>41</sup> seems to be too small to compete with NCX, even considering the lower level of theory used for that prediction. Changing CF<sub>3</sub> groups to cyano groups does not rise the electron affinity but provides nitrogen atoms as safe protonation sites. However, PBE0 functional (without ZPE correction) measures the proton affinity of CB<sub>11</sub>(CN)<sub>12</sub><sup>-</sup> as high as 10.366 eV, while for NCX<sup>-</sup> the same level of theory gives 9.681 eV, so our superhalogen acid is again beyond reach.

The last idea was to use our superhalogen itself as an electron-withdrawing group, a concept applied in other form in hyperhalogens. We took boron as a central atom extending the analogy to hydrofluoric (moderately strong) and tetrafluoroboric (very strong) acids. While B—N bonds are strong enough to make boron nitride almost as hard as diamond, we can expect stability of the "tetrasuperhalogenoborate" anion  $B[NCX]_4^-$  (Figure 9). Its ground state appeared to be a singlet of  $T$  symmetry with surprisingly short B—N bonds of 1.517Å.

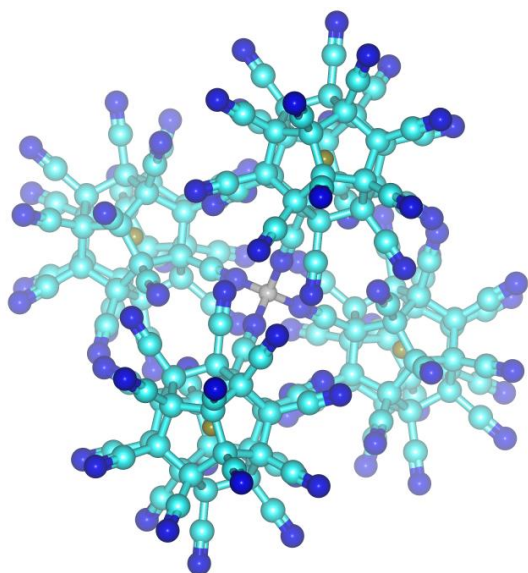


**Figure 9.** Structure of  $B[NCX]_4^-$  anion. Color coding: B – silver, C – cyan, N – dark blue, F – olive.

Unfortunately, this structure was too big for us to handle it with DLPNO-CCSD(T), say nothing about the possible ways of decomposition. However, Hartree-Fock HOMO energy for  $B[NCX]_4^-$  is 1.21 eV lower than for  $NCX^-$ , providing the hope for record-breaking electron affinity around 12 eV for  $B[NCX]_4$ . The latter molecule in its ground state seems to have  $D_2$  symmetry, although we did not calculate harmonic frequencies for that structure to ensure this. As for proton affinity,

there's little chance for  $B[NCX]_4^-$  to make a new record because of bridge-like protonation: the proton in  $HB[NCX]_4$  sticks between two CN needles of adjoining cages.

Thus, to our knowledge,  $HNCX$  should be the strongest stable neutral Brønsted acid ever designed, while  $NCX$  should be the most active superhalogen ever designed, although it may be surpassed by  $B[NCX]_4$ .

### 3. Superalkali and Superbase

#### 3.1. Design.

Tetramethylammonium is known as a good example of non-electrophilic cation, so the corresponding neutral molecule would have stand as a superalkali if it had not lose a methyl radical. Replacing methyl groups with *tert*-butyl ones and then fusing a few six-membered rings prevented the cleavage of C—N bond and finally led to the chiral structure  $NC_{30}H_{36}$  of *T* symmetry (Figure 10). Hereinafter we abbreviate it as **BH**, where **B** is obtained when a hydrogen atom is removed from a tertiary carbon atom.

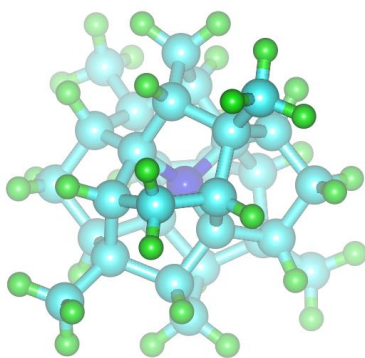


**Figure 10.** Structure of *T*- $NC_{30}H_{36}$ . Color coding: C – cyan, N – blue, H – green.

The framework of **BH** appeared to be a part of so-called "polytope 240".<sup>46</sup> The polytope is regular in positive-curved space, but the projection into flat space makes central bonds shorter than outer bonds, so the nitrogen atom fits the framework quite well because of its smaller covalent radius.

At first sight, the structure of **BH**<sup>+</sup> seems to be quite difficult to build. However, polycyclic quaternary ammonium salts have been known since 1953.<sup>47-49</sup> Recently the interest to them was raised because of their possible usage as phase-transfer catalysts<sup>50</sup>, anion-exchange membranes<sup>51</sup> or electrolytes<sup>52, 53</sup>, inspiring the search of new synthesis techniques which may eventually appear.

### 3.2. Computational details.

As well as for the superhalogen, we used PBE0 for geometry optimizations and zero-point energy estimations, and DLPNO-CCSD(T) for the most of single-point calculations. For energy comparisons involving open-shell systems (e.g., ionization energies) we used UHF wavefunctions and TightPNO cutoffs; otherwise, we used RHF wavefunctions and NormalPNO cutoffs.

A bunch of diffuse functions was manually added to the standard cc-pVTZ basis set for accurate description of the lowest unoccupied molecular orbitals of superalkali. Hydrogens were augmented with four single exponents (0.03s, 0.01s; 0.1p, 0.03p) to deal with near-surface region; the central atom was augmented with ten single exponents (0.03s, 0.01s, 0.003s, 0.001s; 0.03p, 0.01p, 0.003p; 0.02d, 0.004d; 0.005f) for outer regions. AutoAux technique<sup>54</sup> was used to build an auxiliary basis set.

### 3.3. Properties of the superalkali.

According to PBE0 functional, the ground state of **BH**<sup>+</sup> cation is a closed-shell singlet of *T* symmetry with N—C bond lengths of 1.521 Å (about 2% longer than in tetramethylammonium).

The HOMO-LUMO gap of  $\text{BH}^+$  is large, and LUMO matches the symmetry of the molecule, so  $T$  symmetry is retained for both neutral  $\text{BH}$  radical and singlet  $\text{BH}^-$  anion.

DLPNO-CCSD(T) level of theory suggests that ionization energy of neutral  $\text{BH}$  is twice lower than of caesium atom, while electron affinity is only a bit lower (Table 11).

**Table 11.** Ionization energy and electron affinity of  $\text{BH}$ .

Source	IE( $\text{BH}$ ) / eV	EA( $\text{BH}$ ) / eV
PBE0	2.123	0.314
PBE0 ZPE correction	0.048	-0.008
DLPNO-CCSD	1.854	0.317
DLPNO-CCSD(T)	1.899	0.447
DLPNO-CCSD(T) + ZPE	<b>1.947</b>	<b>0.439</b>

We also considered the possible triplet states for  $\text{BH}^-$  anion,  $^3\text{B}_3$  with  $D_2$  symmetry and  $^3\text{A}$  with  $C_3$  symmetry. Both of them appeared below the singlet under DFT, but higher level of theory and ZPE correction (surprisingly high for  $C_3$ -symmetry triplet) qualified them as excited states (Table 12).

**Table 12.** Adiabatic excitation energies of  $\text{BH}^-$  anion.

Source	$E(^1\text{A}_1 \rightarrow ^3\text{B}_3)$ / eV	$E(^1\text{A}_1 \rightarrow ^3\text{A})$ / eV
PBE0	-0.018	-0.012
PBE0 ZPE correction	-0.006	0.145
DLPNO-CCSD	-0.044	-0.052
DLPNO-CCSD(T)	0.079	0.065

DLPNO-CCSD(T) + ZPE	<b>0.073</b>	<b>0.211</b>
---------------------	--------------	--------------

The SOMO in neutral **BH** outspreads far away from its covalent core (Figure 11) suggesting the possibility of metallic bonding between **BH** units. Assuming a body-centered cubic lattice like in alkali metals, we roughly estimated some properties of that metallic phase basing on molecular calculations of **BH** and **[BH]<sub>2</sub>** at PBE0 level of theory.

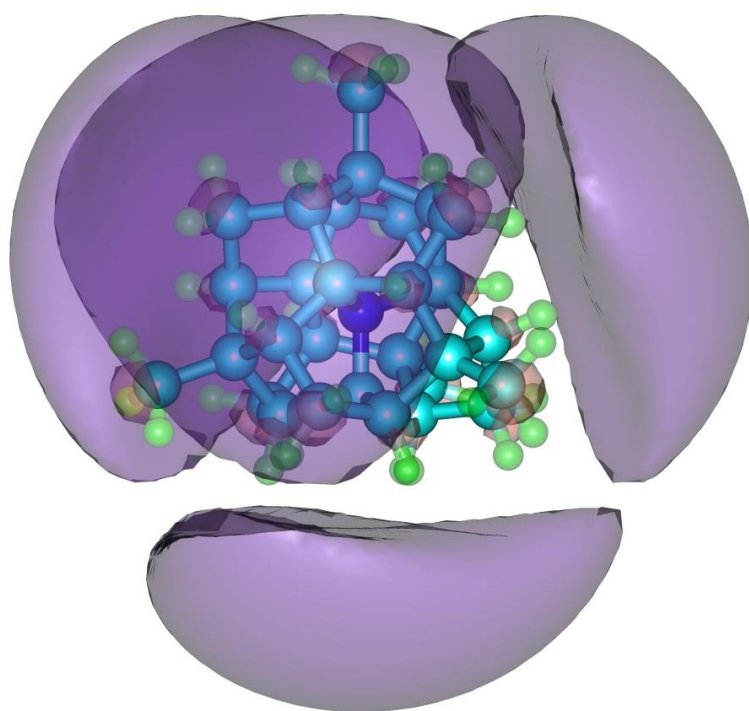


**Figure 11.** SOMO of neutral **BH**. Color coding: C – cyan, N – blue, H – green.

Superalkali dimer **[BH]<sub>2</sub>** has  $D_3$  symmetry (Figure 12) with "bond length" (i.e. the equilibrium distance between the central nitrogens) of 10.025Å. The smallest center-spanning interatomic distance in **[BH]<sub>2</sub>** is 4.285Å between the hydrogens on tertiary carbons. Disregarding ZPE correction, the dissociation energy of the dimer is 0.266 eV, and the ionization energy of **[BH]<sub>2</sub>** is

0.409 eV lower than of **BH**. Therefore  $[\mathbf{BH}]_2$  outperforms the so-called "ditungsten tetra(hpp)"<sup>55</sup>, known as the most easily ionized closed-shell molecule<sup>56</sup>, more than twice.

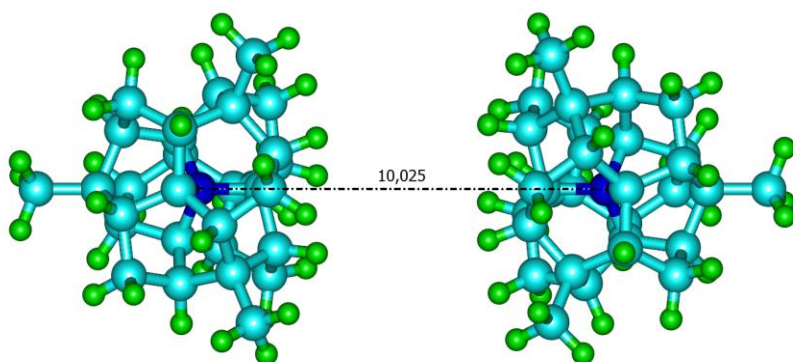


**Figure 12.** Structure of  $[\mathbf{BH}]_2$  dimer. Color coding: C – cyan, N – blue, H – green.

The lattice parameter  $a_{bcc}$  of alkali metals at 20°C closely corresponds to the equilibrium internuclear distance  $r_e$  in their diatomic molecules (Figure 13). The mean ratio  $a_{bcc} / r_e$  is about 1.357, so the lattice parameter of **BH** metal was estimated as  $1.357 \cdot 10.025 \text{ \AA} \approx 13.6 \text{ \AA}$ , leading to bulk density of  $0.54 \text{ g/cm}^3$ . The corresponding space group should be  $I23$ .

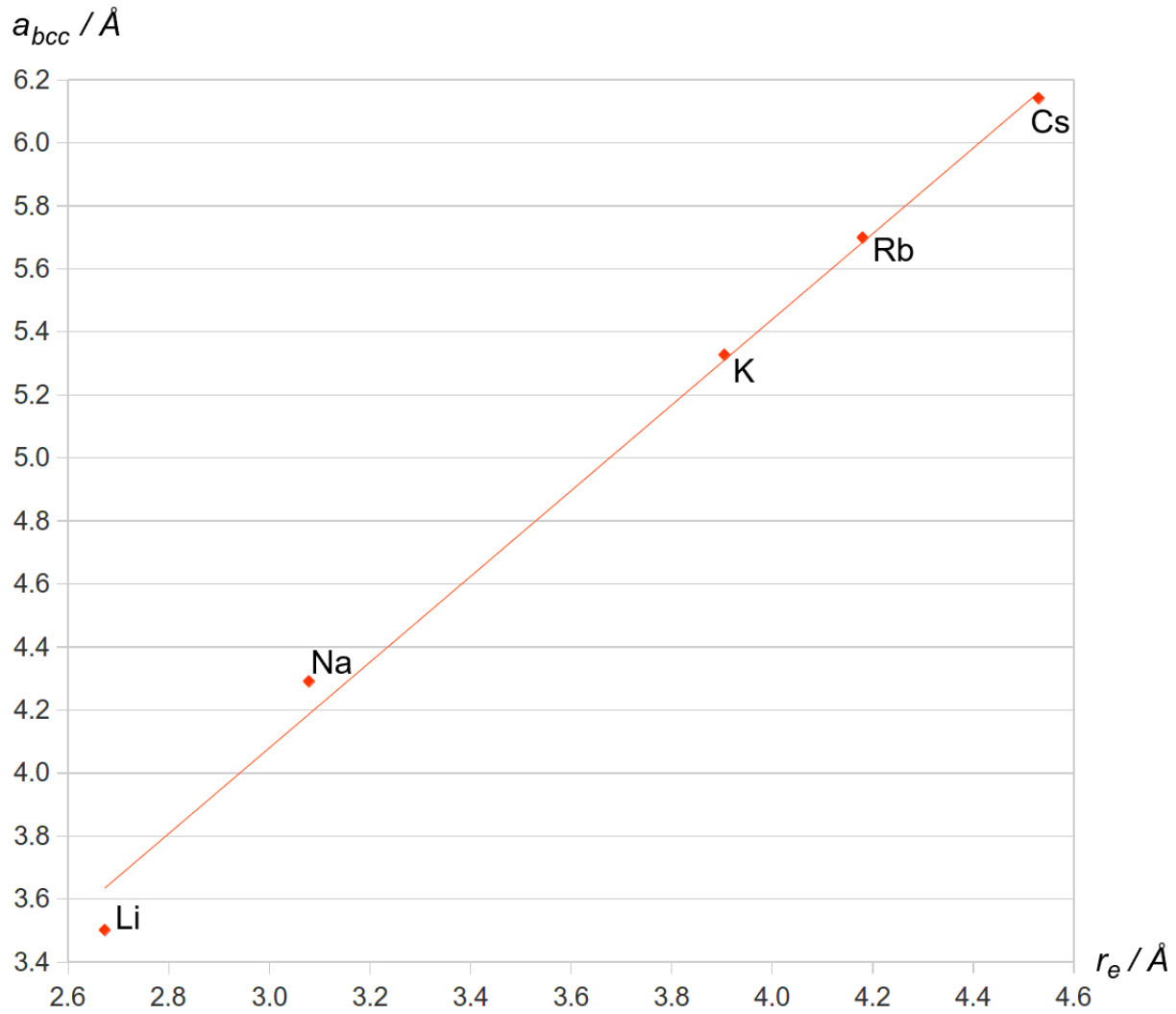


**Figure 13.** Correlation between lattice parameter ( $a_{bcc}$ ) and internuclear distance in diatomic molecules ( $r_e$ ) for alkali metals. The data was taken from reference books.

Using a similar correlation between the work function and the sum of ionization energy and electron affinity for alkali metals, the work function of **BH** metal at 20°C was estimated as  $0.46 \cdot (\text{IE} + \text{EA}) \approx 1.1$  eV, nearly approaching the current record for a composite material<sup>57</sup>.

Heavy alkali metals are known to be fairly transparent to near ultraviolet because of the low plasmonic energies  $E_P$ , corresponding to the Langmuir waves in electron gas. The theoretical value

of plasmonic energy may be calculated as  $E_p^{th} = \hbar e \sqrt{\frac{n_e}{m_e \epsilon_0}}$  where  $e$  is the elementary charge,  $m_e$  is the electron mass and  $n_e$  is the formal concentration of conduction electrons, i.e. two electrons per unit cell for alkali metals.  $E_p^{th}$  is usually greater than the experimental value  $E_p^{exp}$ , so we plotted the ratio  $E_p^{exp}/E_p^{th}$  against the sum  $IE + EA$  and found some correlation (Figure 14). It provided a crude estimate of  $E_p \approx 0.73$  eV for **BH** metal, so it is expected to be notably transparent for wavelengths up to  $\sim 1700$  nm.

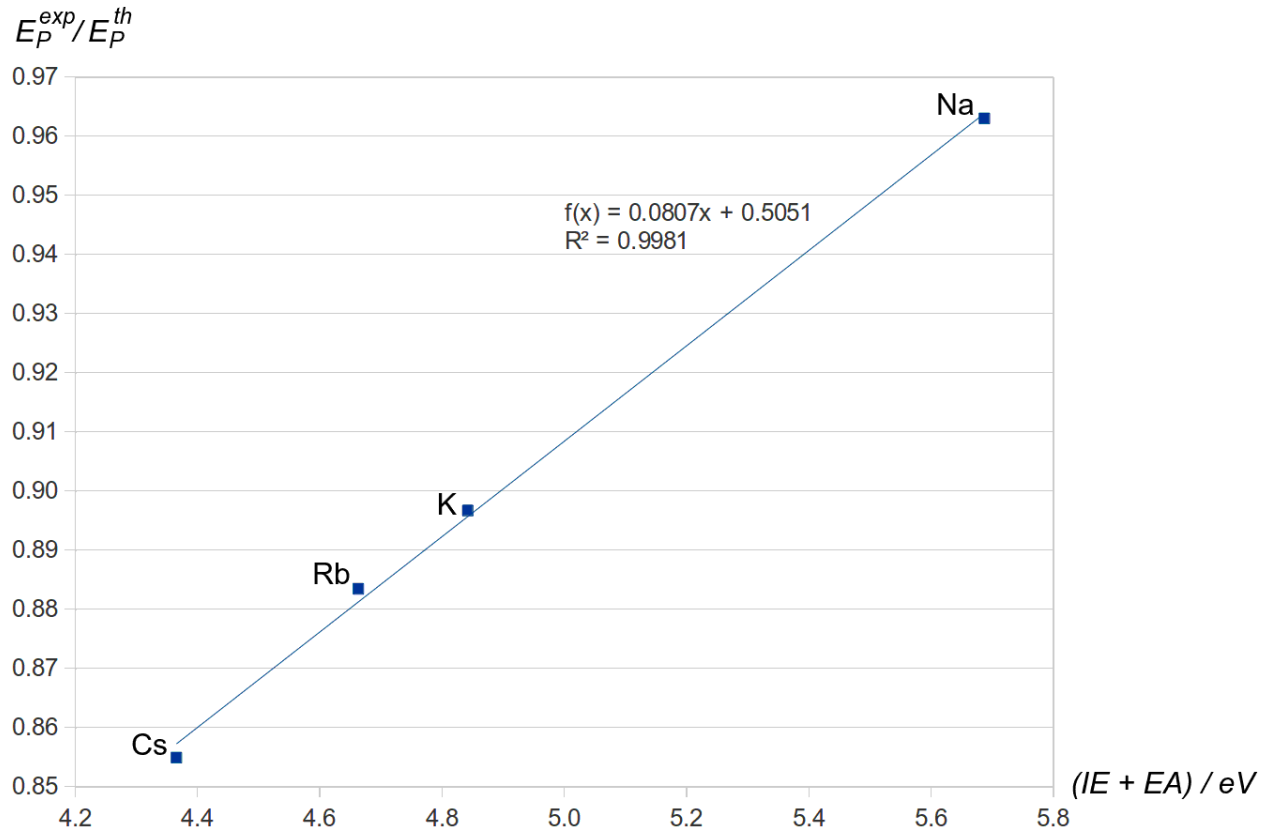


**Figure 14.** Correlation between the scaled plasmonic energy ( $E_p^{exp}/E_p^{th}$ ) and the sum of ionization energy and electron affinity ( $IE + EA$ ) for alkali metals.

The chirality of **BH** units suggests a possibility of magnetochiral anisotropy<sup>58, 59</sup> for **BH** metal.

### 3.4. Superbase.

As well as the protonation of a superhalogen anion leads to superacid, the deprotonation of a superalkali cation leads to superbase. Tertiary carbon is the most favorable deprotonation site in  $\mathbf{BH}^+$  cation, so our superbase is just  $\mathbf{B}$ . Once deprotonated, that carbon forms a double bond with a deeper carbon, pulling it out from nitrogen, which stays with a lone electron pair (Figure 15). That double bond cannot be planar because of structure rigidity, so the overall process appeared to be quite endothermic (Table 13).

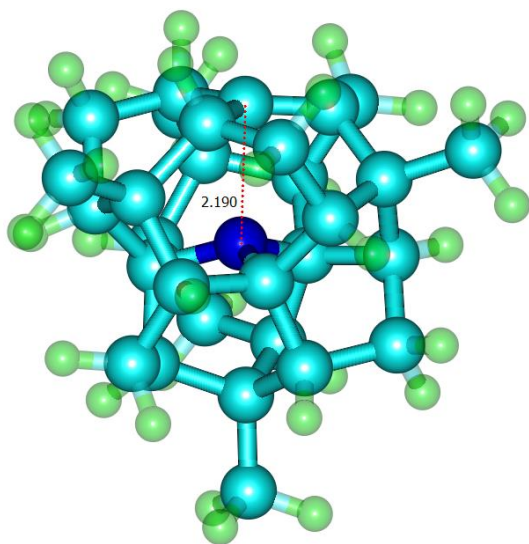


**Figure 15.** Structure of superbase  $\text{NC}_{30}\text{H}_{35}$ . Color coding: C – cyan, N – blue, H – green.

We also compared  $\mathbf{B}$  to one of the strongest known neutral Brønsted bases (Figure 16), labeled 32a by Reinhard Schwesinger in his paper<sup>60</sup>, hereinafter abbreviated  $\mathbf{RS}$ . The conformations of  $\mathbf{RS}$  and  $\mathbf{RSH}^+$  are the lowest we could find using Figure 2 from Schwesinger's paper as a starting point. Although they were not strictly proven to be ground minima in the gas phase, at least they are close



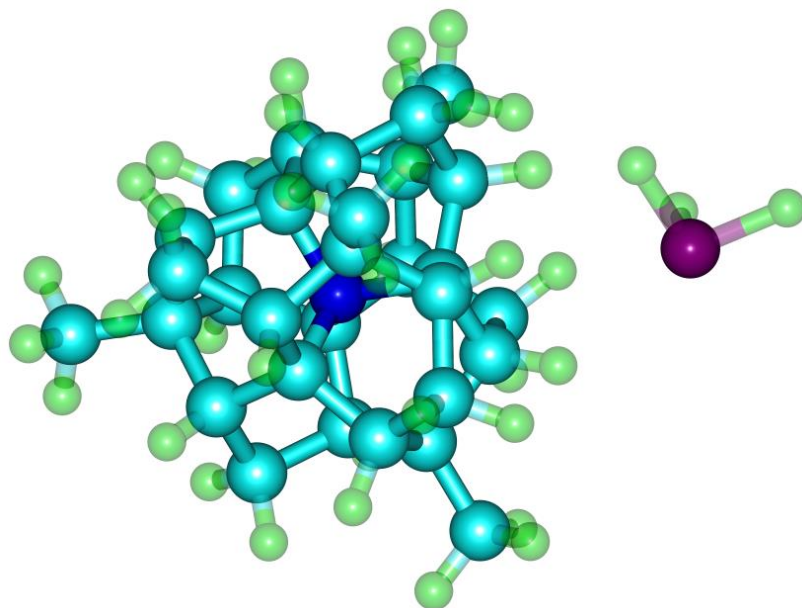


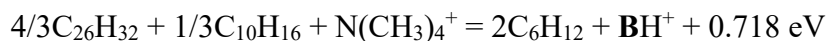
**Figure 17.** Ion pair  $\text{BH}^+\text{SiH}_3^-$  as a result of silane deprotonation by **B**. Color coding: C – cyan, N – blue, H – transparent green, Si – magenta.

### 3.5. Stability.

The total strain of  $\text{BH}^+$  structure was examined at PBE0/cc-pVTZ level of theory (with ZPE correction) using two homodesmotic reactions. First of them is a classical one, involving alkanes from  $\text{C}_2$  to  $\text{C}_5$  for different types of carbon atoms:



Second one is more specific and involves diamondoids  $\text{C}_{10}\text{H}_{16}$  (adamantane) and  $\text{C}_{26}\text{H}_{32}$  ( $T_d$ -pentamantane) along with cyclohexane:



Taking into account that there are 31 heavy atoms in the structure, we see that the total strain is about 0.5 kcal/mol per atom, so the framework should be stable against skeleton rearrangements.

The loss of hydrogen is another possible way of **BH** destruction:



That reaction is a bit exothermic (DLPNO-CCSD(T) + ZPE), but strong C—H and H—H bonds should make the total process kinetically inhibited. It is quite likely that metallic palladium could be a proper catalyst here, so the reduction of **BH**<sup>+</sup> on the palladium cathode might release hydrogen gas yielding a pure superbase **B**.

### 3.6. Possible improvements.

A straightforward way to reduce the ionization energy is to replace the central nitrogen with phosphorus while enlarging the whole structure. Hence we attached four bicyclo[2.2.2]octane units to the phosphorus atom, fused them with six isopropylidene locks, and finally added four methyl groups on outer tertiary carbons just like in **BH**, achieving superalkali PC<sub>54</sub>H<sub>84</sub> (Figure 18). The structure has *T* symmetry in both neutral and cationic forms.

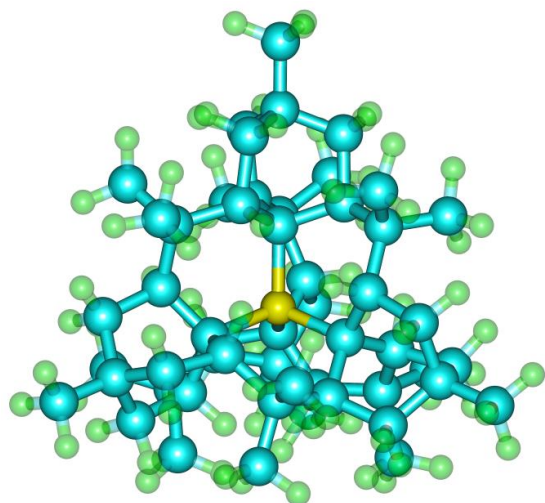


**Figure 18.** Structure of superalkali  $\text{PC}_{54}\text{H}_{84}$ , a possible successor of **BH**. Color coding: C – cyan, H – transparent green, P – yellow.

For  $\text{PC}_{54}\text{H}_{84}$  we used cc-pVTZ basis set augmented the same way as for **BH**. According to PBE0 functional, the central P—C bond length appeared to be 1.846Å for cation and 1.847Å for neutral molecule (that is almost 3% longer than in tetramethylphosphonium). The ionization energy was estimated to be 0.277 eV lower for  $\text{PC}_{54}\text{H}_{84}$  compared to **BH**, so its dimer  $[\text{PC}_{54}\text{H}_{84}]_2$  could probably dive below 1.4 eV. Concerning stability, it seems that long P—C bonds could be fragile, although they are sterically hindered, so the structure could still survive at room temperature. As for metallic phase analogous to **BH** metal, it is questionable because of the large size of  $\text{PC}_{54}\text{H}_{84}$  units.

The first step to improve the basicity was an idea of dodecahedrane cage with a sodium cation inside. Feeding such a cage with 20 methyl groups, we obtain quite robust permethyl-dodecahedrane complex of  $I_h$  symmetry that is very hard to deprotonate. The corresponding superbase,  $\text{Na}@C_{20}(\text{CH}_3)_{19}\text{CH}_2$ , has a singlet ground state of  $C_s$  symmetry with one of the cage C—C bonds stretched to 1.718Å, while the protonated structure has cage bond lengths of 1.608Å (Figure 19). That high strain is barely a problem in the sense of stability, but could be a problem for synthesis. Nevertheless, the calculated proton affinity of that superbase is 14.375 eV (PBE0 + ZPE), while lithium analogue is a bit less basic (14.342 eV). The standard cc-pVTZ basis set was used because of negligible influence of diffuse functions on the PA calculations (as shown in Table 13).

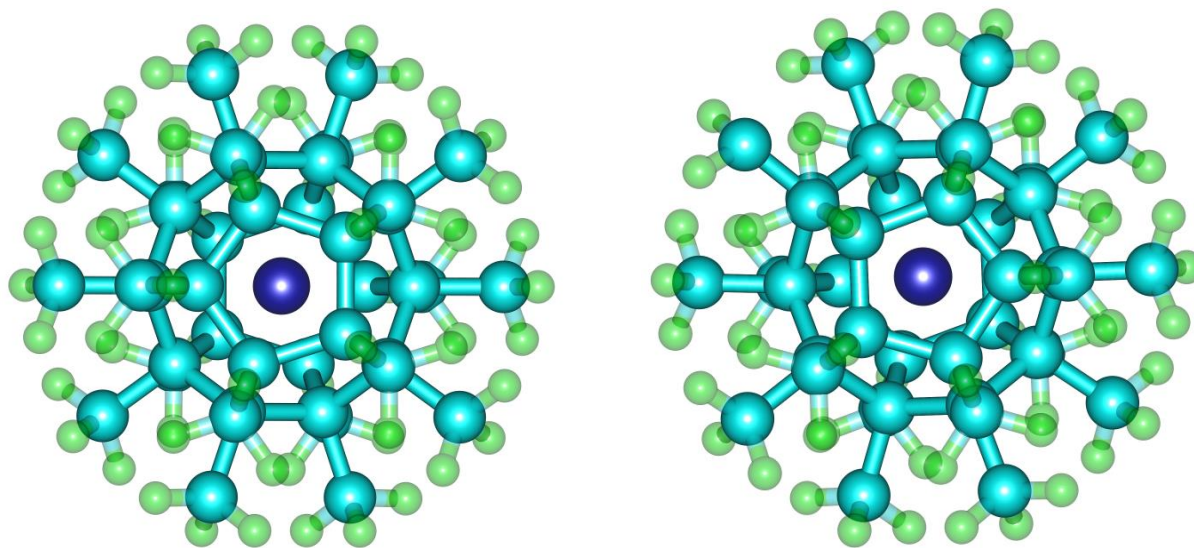


**Figure 19.** Structure of superalkali  $\text{Na}@C_{20}(\text{CH}_3)_{20}$  (left) and the corresponding superbase  $\text{Na}@C_{20}(\text{CH}_3)_{19}\text{CH}_2$  (right). Color coding: C – cyan, Na – dark blue, H – transparent green.

Both neutral  $\text{Na}@C_{20}(\text{CH}_3)_{20}$  and  $\text{Li}@C_{20}(\text{CH}_3)_{20}$  feature the same  $I_h$  symmetry as cations do. PBE0 with manually augmented cc-pVTZ basis set estimated their ionization energies to be 2.115 and 2.146 eV, respectively. These values agree within 0.02 eV to ionization energy of **BH** at the same level of theory, so there is no chance for these cage structures to outperform  $\text{PC}_{54}\text{H}_{84}$ . Their large size and incomprehensible way to synthesize forced us to abandon them and switch to hunting over stronger bases.

### 3.7. The limits of neutral Brønsted organic superbases.

Some theoretical claims of gas-phase basicities of up to 348 kcal/mol were reported by Ilmar Koppel<sup>61</sup> in 2014 and then developed by Ivo Leito and coworkers in 2015<sup>62</sup>. The corresponding proton affinities go beyond 16 eV, so we took a look at the molecules suggested there. They have the same structural motif, a phosphazene chain similar to one in **RS** superbase, but  $\text{N}(\text{CH}_2)_4$  groups

are replaced with 2,5-dimethylimidazolidino (imme) groups, while the nitrogen atom to be protonated is replaced with CH group or even with a divalent carbon atom.

Unfortunately, a closer look at the most basic structures from Scheme 2 in Ref. <sup>62</sup> revealed their instability. For example, in the molecule  $t\text{-Bu}-\text{CH}=\text{P}(\text{imme})_3$ , labeled there "300.0", a methyl group from imme attacks the  $\text{C}=\text{P}$  double bond (Figure 20). Intrinsically, that methyl group becomes the most favorable deprotonation site in the cation, so the above-described process becomes more exothermic for stronger bases of that type. Another problem turned up for carbene bases: e.g., in the molecule labeled "311.0",  $(\text{imme})-\text{C}=\text{N}=\text{P}(\text{imme})_3$ , the carbene atom is attacked either by a methyl group from imme or by a "guanidinic" carbon (Figure 21). The latter process occurs without any barrier during geometry optimization procedure, although the Supporting Information of Ref <sup>62</sup> says that the most stable conformers of each species were found.

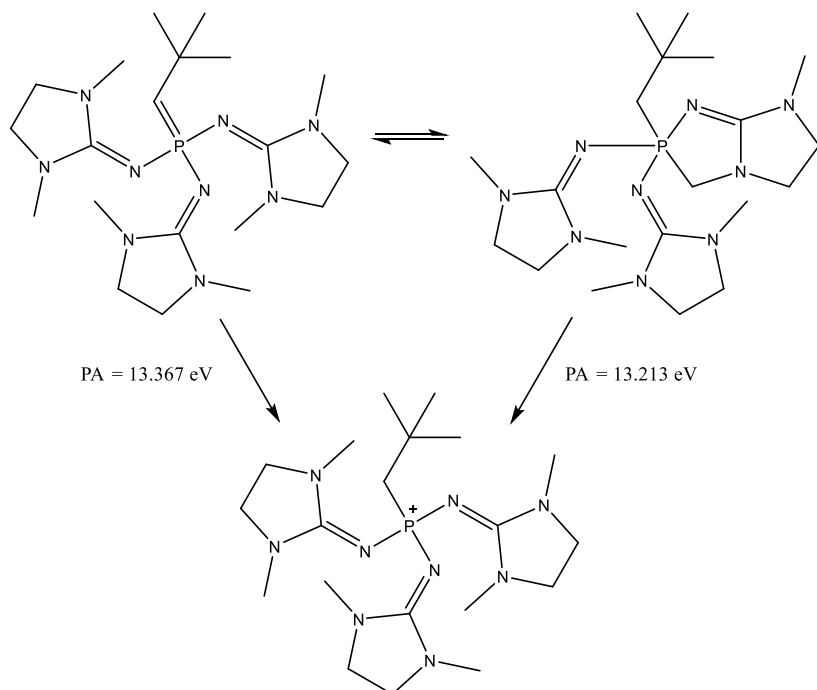


**Figure 20.** Protonation of  $t\text{-Bu}-\text{CH}=\text{P}(\text{imme})_3$  and its more stable tautomer, DLPNO-CCSD(T)

+ ZPE

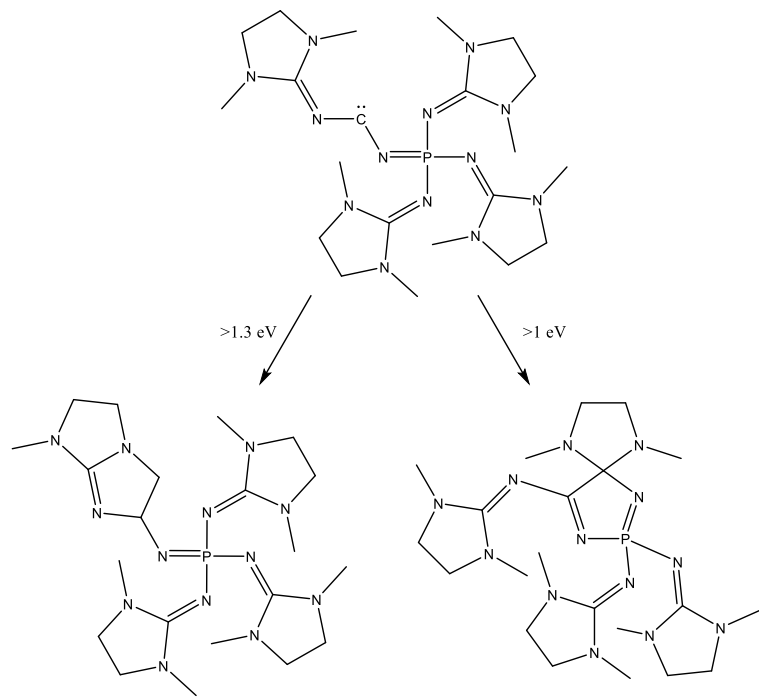


**Figure 21.** Instability of  $(\text{imme})-\text{C}-\text{N}=\text{P}(\text{imme})_3$ .

These stability issues might explain why the record-breaking bases of that type did not appear experimentally<sup>63,64</sup>. However, to prove that the very notion of a phosphazene-like superbase is not completely hopeless, we designed a stable superbase, named **PZ**, with proton affinity above 15 eV. Its protonated form is shown on Figure 22.

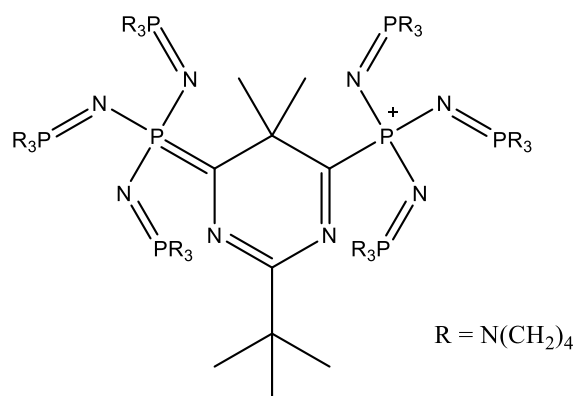


**Figure 22.** Protonated form of phosphazene-like superbase **PZ**.

The favorite deprotonation site in **PZH**<sup>+</sup> is the secondary carbon next to nitrogen in N(CH<sub>2</sub>)<sub>4</sub> group (rotations and nitrogen inversions make all these carbons equivalent), that corresponds to the tautomer **PZ**. Second feasible site is the primary carbon attached to the central ring, that tautomer is named **PZ'**.

**Table 14.** Proton affinity of **PZ** and its tautomer **PZ'**.

Source	PA( <b>PZ</b> ) / eV	PA( <b>PZ'</b> ) / eV
PBE0 <sup>a</sup>	15.571	15.821
PBE0 ZPE correction <sup>a</sup>	-0.475	-0.484
DLPNO-CCSD	15.631	15.963
DLPNO-CCSD(T)	15.536	15.695
DLPNO-CCSD(T) + ZPE	<b>15.060</b>	<b>15.211</b>

<sup>a</sup> Performed with 6-311G\* basis set.

As well as for **RS** base, the conformations found for **PZ**, **PZ'** and **PZH<sup>+</sup>** were not strictly proven to be global minima, but at least they are the lowest we could find.

**PZ** superbases look quite synthesizable instead of crazy dodecahedrane cages mentioned in the previous section. Its proton affinity outperforms the strongest Schwesinger's superbase by 1.65 eV, i.e. **PZ** is about 28 orders of magnitude stronger than **RS**. But the deprotonation of such weakly acidic groups as  $\text{N}(\text{CH}_2)_4$  makes further improvements doubtful. It seems that proton affinity of 15 eV is right below the limit for stable neutral Brønsted superbases.

An obvious vulnerability area in **PZ** is the bond between the central cycle and the phosphorus atom. The substitution of that phosphorus by deprotonated carbon was estimated to be exothermic by more than 1 eV (Figure 23), but steric hindrance should provide significant kinetic stability here.

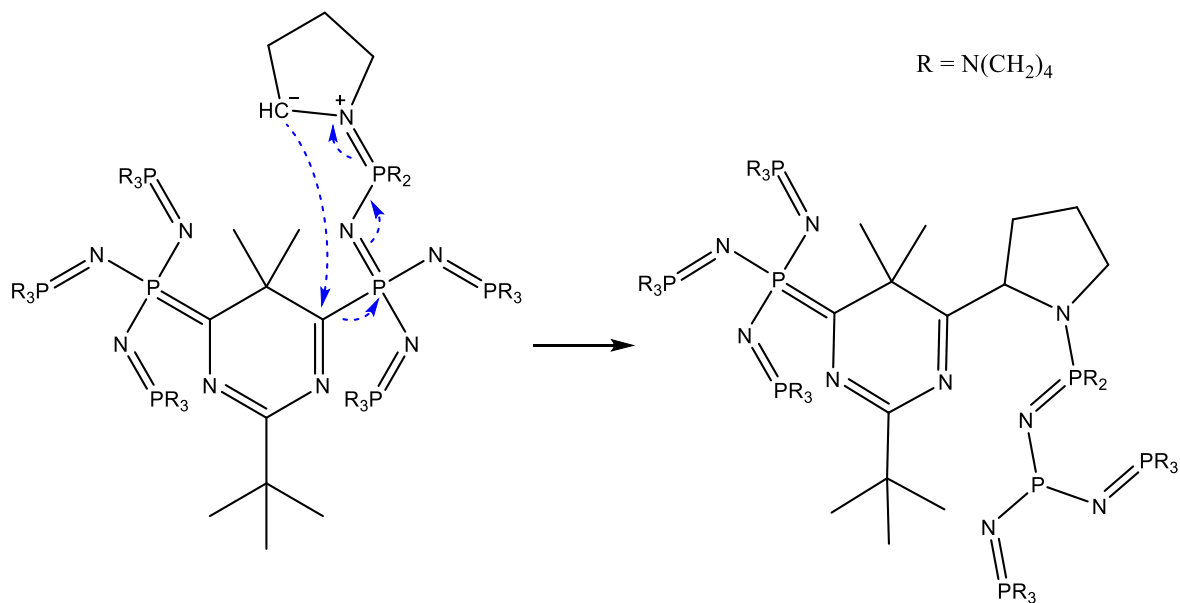


**Figure 23.** A possible way of **PZ** destruction.

Even more basic structures were considered while designing **PZ**, but all of them looked unstable as compounds. For example, if a *tert*-butyl cation is removed from **PZH**<sup>+</sup>, then the bared carbon will be protonated as exothermically as 16 eV. Furthermore, if we replace the nitrogens in the central cycle with BCH<sub>3</sub> groups, and the adjacent carbons with nitrogens, the proton affinity will rise to astonishing 17 eV (Figure 24). Such a structure would still be stable as a single molecule, but self-deprotonation would be unavoidable for a compound.

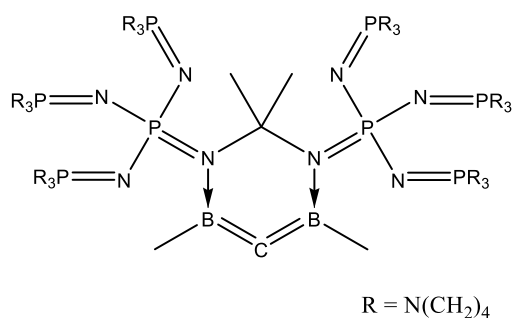


**Figure 24.** A stable molecule with a proton affinity of 17 eV (the protonation site is the carbon atom between two boron atoms).

#### 4. Conclusions

We designed a superhalogen F@C<sub>20</sub>(CN)<sub>20</sub>, named **NCX**, with electron affinity of 10.8 eV, the highest (to our knowledge) ever predicted for a neutral molecule, and considered some of its derivatives: a fluorine superhalogenide **FNCX**, a superhalogen dimer [**NCX**]<sub>2</sub>, a hyperhalogen B[**NCX**]<sub>4</sub> with electron affinity close to 12 eV, and a superacid **HNCX** with gas-phase deprotonation energy of just 9.3 eV. Being much stronger acid than the current champion, fluorocarborane acid, **HNCX** is expected to have a high degree of autoionization in condensed phase, and to be close to protonation of molecular nitrogen. Both **HNCX** and **NCX**<sup>-</sup> anion were

predicted to be thermodynamically stable against cyanide loss, while neutral NCX is expected to have only kinetic stability.

We designed a superalkali NC<sub>30</sub>H<sub>36</sub>, named **BH**, with ionization energy of about 1.9 eV, the lowest (to our knowledge) ever predicted for a neutral molecule, and considered a metallic phase formed by **BH** units. Assuming a body-centered cubic lattice common for alkali metals, we predicted **BH** metal to have *I23* space group with  $a = 13.6\text{\AA}$  corresponding to bulk density of 0.54 g/cm<sup>3</sup>, work function of about 1.1 eV and plasmonic energy of about 0.73 eV leading to transparency for wavelengths up to ~1700 nm. The skeleton strain and the stability against hydrogen loss was checked for **BH**. The corresponding superbase **B** was shown to outperform the current champion, Schwesinger's base, easily deprotonating silane.

We drowned the limits of ionization energy for neutral molecules to about 1.4 eV with related structure PC<sub>54</sub>H<sub>84</sub> and its dimer. We also checked the limits of phosphazene-like bases, designing a stable neutral Brønsted superbase with gas-phase proton affinity above 15 eV, outperforming Schwesinger's base by about 28 orders of magnitude.

Various ways of possible improvements to superhalogens and superalkali were investigated. The instability of some earlier-claimed superacids and superbases of record strength was established.

#### ASSOCIATED CONTENT

**Supporting Information.** XYZ coordinates and total energies for the most of discussed structures are available free of charge via the Internet at <http://pubs.acs.org>.

#### AUTHOR INFORMATION

##### Corresponding Authors

\* Andrey V. Kulsha [Andrey\\_601@tut.by](mailto:Andrey_601@tut.by)

\* Dmitry I. Sharapa [dmitry.sharapa@kit.edu](mailto:dmitry.sharapa@kit.edu)

## ORCID

Andrey V. Kulsha [0000-0001-5068-7101](https://orcid.org/0000-0001-5068-7101)

Dmitry I. Sharapa [0000-0001-9510-9081](https://orcid.org/0000-0001-9510-9081)

## Present Addresses

†Current contact address of D.I.S is Institute of Catalysis Research and Technology (IKFT),  
Hermann-von-Helmholtz-Platz 1, D-76344 Eggenstein-Leopoldshafen, Germany

## Author Contributions

The manuscript was written through contributions of both authors. Both authors have given approval to the final version of the manuscript. ‡Both authors contributed equally (computations by D.I.S., design by A.V.K.).

## ACKNOWLEDGMENT

D. I. S. would like to thank Deutsche Forschungsgemeinschaft (DFG-SFB 953 “Synthetic Carbon Allotropes”).

## ABBREVIATIONS

PA, proton affinity; EA, electron affinity; IE, ionization energy; DE, dissociation energy; ZPE, zero-point energy

## REFERENCES

1. Craciun, R.; Picone, D.; Long, R. T.; Li, S.; Dixon, D. A.; Peterson, K. A.; Christe, K. O., Third Row Transition Metal Hexafluorides, Extraordinary Oxidizers, and Lewis Acids: Electron

- Affinities, Fluoride Affinities, and Heats of Formation of WF<sub>6</sub>, ReF<sub>6</sub>, OsF<sub>6</sub>, IrF<sub>6</sub>, PtF<sub>6</sub>, and AuF<sub>6</sub>. *Inorganic Chemistry* **2010**, *49* (3), 1056-1070.
2. Yokoyama, K.; Tanaka, H.; Kudo, H., Structure of Hyperlithiated Li<sub>3</sub>O and Evidence for Electronomers. *The Journal of Physical Chemistry A* **2001**, *105* (17), 4312-4315.
  3. Maksić, Z. B.; Kovačević, B.; Vianello, R., Advances in Determining the Absolute Proton Affinities of Neutral Organic Molecules in the Gas Phase and Their Interpretation: A Theoretical Account. *Chemical Reviews* **2012**, *112* (10), 5240-5270.
  4. Rienstra-Kiracofe, J. C.; Tschumper, G. S.; Schaefer, H. F.; Nandi, S.; Ellison, G. B., Atomic and Molecular Electron Affinities: Photoelectron Experiments and Theoretical Computations. *Chemical Reviews* **2002**, *102* (1), 231-282.
  5. Raczynska Ewa, D.; Decouzon, M.; Gal, J. F.; Maria, P. C.; Wozniak, K.; Kurg, R.; Carins Stuart, N., ChemInform Abstract: Superbases and Superacids in the Gas Phase. *ChemInform* **2010**, *31* (33).
  6. Srivastava, A. K.; Misra, N., Superbases and superacids form supersalts. *Chemical Physics Letters* **2016**, *644*, 1-4.
  7. Srivastava, A. K., Organic superalkalis with closed-shell structure and aromaticity. *Molecular Physics* **2018**, *116* (12), 1642-1649.
  8. Nava, M.; Stoyanova Irina, V.; Cummings, S.; Stoyanov Evgenii, S.; Reed Christopher, A., The Strongest Brønsted Acid: Protonation of Alkanes by H(CHB11F11) at Room Temperature. *Angewandte Chemie International Edition* **2013**, *53* (4), 1131-1134.
  9. Zhao, H.; Zhou, J.; Jena, P., Stability of B<sub>12</sub>(CN)<sub>12</sub><sup>-</sup>: Implications for Lithium and Magnesium Ion Batteries. *Angewandte Chemie International Edition* **2016**, *55* (11), 3704-3708.
  10. Riplinger, C.; Neese, F., An efficient and near linear scaling pair natural orbital based local coupled cluster method. *The Journal of Chemical Physics* **2013**, *138* (3), 034106.
  11. Riplinger, C.; Sandhoefer, B.; Hansen, A.; Neese, F., Natural triple excitations in local coupled cluster calculations with pair natural orbitals. *The Journal of Chemical Physics* **2013**, *139* (13), 134101.
  12. Liakos, D. G.; Sparta, M.; Kesharwani, M. K.; Martin, J. M. L.; Neese, F., Exploring the Accuracy Limits of Local Pair Natural Orbital Coupled-Cluster Theory. *Journal of Chemical Theory and Computation* **2015**, *11* (4), 1525-1539.
  13. Liakos, D. G.; Neese, F., Is It Possible To Obtain Coupled Cluster Quality Energies at near Density Functional Theory Cost? Domain-Based Local Pair Natural Orbital Coupled Cluster vs Modern Density Functional Theory. *Journal of Chemical Theory and Computation* **2015**, *11* (9), 4054-4063.
  14. Riplinger, C.; Pinski, P.; Becker, U.; Valeev, E. F.; Neese, F., Sparse maps—A systematic infrastructure for reduced-scaling electronic structure methods. II. Linear scaling domain based pair natural orbital coupled cluster theory. *The Journal of Chemical Physics* **2016**, *144* (2), 024109.
  15. Saitow, M.; Becker, U.; Riplinger, C.; Valeev, E. F.; Neese, F., A new near-linear scaling, efficient and accurate, open-shell domain-based local pair natural orbital coupled cluster singles and doubles theory. *The Journal of Chemical Physics* **2017**, *146* (16), 164105.
  16. Neese, F., Software update: the ORCA program system, version 4.0. *Wiley Interdisciplinary Reviews: Computational Molecular Science* **2017**, *8* (1), e1327.
  17. Bistoni, G.; Riplinger, C.; Minenkov, Y.; Cavallo, L.; Auer, A. A.; Neese, F., Treating Subvalence Correlation Effects in Domain Based Pair Natural Orbital Coupled Cluster Calculations: An Out-of-the-Box Approach. *J. Chem. Theory Comput.* **2017**, *13* (7), 3220-3227.

18. Guo, Y.; Riplinger, C.; Becker, U.; Liakos, D. G.; Minenkov, Y.; Cavallo, L.; Neese, F., Communication: An improved linear scaling perturbative triples correction for the domain based local pair-natural orbital based singles and doubles coupled cluster method [DLPNO-CCSD(T)]. *J. Chem. Phys.* **2018**, *148* (1), 011101/1-011101/5.
19. Minenkov, Y.; Bistoni, G.; Riplinger, C.; Auer, A. A.; Neese, F.; Cavallo, L., Pair natural orbital and canonical coupled cluster reaction enthalpies involving light to heavy alkali and alkaline earth metals: the importance of sub-valence correlation. *Phys. Chem. Chem. Phys.* **2017**, *19* (14), 9374-9391.
20. Minenkov, Y.; Chermak, E.; Cavallo, L., Accuracy of DLPNO-CCSD(T) Method for Noncovalent Bond Dissociation Enthalpies from Coinage Metal Cation Complexes. *J. Chem. Theory Comput.* **2015**, *11* (10), 4664-4676.
21. Minenkov, Y.; Chermak, E.; Cavallo, L., Troubles in the Systematic Prediction of Transition Metal Thermochemistry with Contemporary Out-of-the-Box Methods. *J. Chem. Theory Comput.* **2016**, *12* (4), 1542-1560.
22. Minenkov, Y.; Sliznev, V. V.; Cavallo, L., Accurate Gas Phase Formation Enthalpies of Alloys and Refractories Decomposition Products. *Inorg. Chem.* **2017**, *56* (3), 1386-1401.
23. Minenkov, Y.; Wang, H.; Wang, Z.; Sarathy, S. M.; Cavallo, L., Heats of Formation of Medium-Sized Organic Compounds from Contemporary Electronic Structure Methods. *J. Chem. Theory Comput.* **2017**, *13* (8), 3537-3560.
24. Dunning, T. H., Gaussian basis sets for use in correlated molecular calculations. I. The atoms boron through neon and hydrogen. *The Journal of Chemical Physics* **1989**, *90* (2), 1007-1023.
25. Papajak, E.; Leverentz, H. R.; Zheng, J.; Truhlar, D. G., Efficient Diffuse Basis Sets: cc-pVxZ+ and maug-cc-pVxZ. *Journal of Chemical Theory and Computation* **2009**, *5* (5), 1197-1202.
26. Weigend, F.; Köhn, A.; Hättig, C., Efficient use of the correlation consistent basis sets in resolution of the identity MP2 calculations. *The Journal of Chemical Physics* **2002**, *116* (8), 3175-3183.
27. Krishnan, R.; Binkley, J. S.; Seeger, R.; Pople, J. A., Self-consistent molecular orbital methods. XX. A basis set for correlated wave functions. *The Journal of Chemical Physics* **1980**, *72* (1), 650-654.
28. Adamo, C.; Barone, V., Toward reliable density functional methods without adjustable parameters: The PBE0 model. *The Journal of Chemical Physics* **1999**, *110* (13), 6158-6170.
29. Frisch, M. J.; Trucks, G. W.; Schlegel, H. B.; Scuseria, G. E.; Robb, M. A.; Cheeseman, J. R.; Scalmani, G.; Barone, V.; Petersson, G. A.; Nakatsuji, H.; Li, X.; Caricato, M.; Marenich, A. V.; Bloino, J.; Janesko, B. G.; Gomperts, R.; Mennucci, B.; Hratchian, H. P.; Ortiz, J. V.; Izmaylov, A. F.; Sonnenberg, J. L.; Williams, J.; Ding, F.; Lipparini, F.; Egidi, F.; Goings, J.; Peng, B.; Petrone, A.; Henderson, T.; Ranasinghe, D.; Zakrzewski, V. G.; Gao, J.; Rega, N.; Zheng, G.; Liang, W.; Hada, M.; Ehara, M.; Toyota, K.; Fukuda, R.; Hasegawa, J.; Ishida, M.; Nakajima, T.; Honda, Y.; Kitao, O.; Nakai, H.; Vreven, T.; Throssell, K.; Montgomery Jr., J. A.; Peralta, J. E.; Ogliaro, F.; Bearpark, M. J.; Heyd, J. J.; Brothers, E. N.; Kudin, K. N.; Staroverov, V. N.; Keith, T. A.; Kobayashi, R.; Normand, J.; Raghavachari, K.; Rendell, A. P.; Burant, J. C.; Iyengar, S. S.; Tomasi, J.; Cossi, M.; Millam, J. M.; Klene, M.; Adamo, C.; Cammi, R.; Ochterski, J. W.; Martin, R. L.; Morokuma, K.; Farkas, O.; Foresman, J. B.; Fox, D. J. *Gaussian 16 Rev. A.01*, Wallingford, CT, 2016.

30. Liakos, D. G.; Sparta, M.; Kesharwani, M. K.; Martin, J. M. L.; Neese, F., Exploring the Accuracy Limits of Local Pair Natural Orbital Coupled-Cluster Theory. *J. Chem. Theory Comput.* **2015**, *11* (4), 1525-1539.
31. Cummings, S.; Hratchian Hrant, P.; Reed Christopher, A., The Strongest Acid: Protonation of Carbon Dioxide. *Angewandte Chemie International Edition* **2016**, *55* (4), 1382-1386.
32. Reed, C. A., Myths about the Proton. The Nature of H<sup>+</sup> in Condensed Media. *Accounts of Chemical Research* **2013**, *46* (11), 2567-2575.
33. Verdes, D.; Linnartz, H.; Maier, J. P.; Botschwina, P.; Oswald, R.; Rosmus, P.; Knowles, P. J., Spectroscopic and theoretical characterization of linear centrosymmetric N≡N·H<sup>+</sup>·N≡N. *The Journal of Chemical Physics* **1999**, *111* (18), 8400-8403.
34. Webster, O. W., Polycyanation. The Reaction of Cyanogen Chloride, Cyclopentadiene, and Sodium Hydride. *Journal of the American Chemical Society* **1966**, *88* (13), 3046-3050.
35. Eckert, F.; Leito, I.; Kaljurand, I.; Kütt, A.; Klamt, A.; Diedenhofen, M., Prediction of acidity in acetonitrile solution with COSMO-RS. *Journal of Computational Chemistry* **2009**, *30* (5), 799-810.
36. Hu, Q. J.; Hepburn, J. W., Energetics and dynamics of threshold photoion-pair formation in HF/DF. *The Journal of Chemical Physics* **2006**, *124* (7), 074311.
37. Christophe, B.; Christian, D.; Fabienne, G., Electron spectrometry at the μeV level and the electron affinities of Si and F. *Journal of Physics B: Atomic, Molecular and Optical Physics* **2001**, *34* (9), L281.
38. Cross, R. J.; Saunders, M.; Prinzbach, H., Putting Helium Inside Dodecahedrane. *Organic Letters* **1999**, *1* (9), 1479-1481.
39. Irikura, K. K., In-Adamantane, a Small Inside-Out Molecule. *The Journal of Organic Chemistry* **2008**, *73* (20), 7906-7908.
40. Bradforth, S. E.; Kim, E. H.; Arnold, D. W.; Neumark, D. M., Photoelectron spectroscopy of CN<sup>-</sup>, NCO<sup>-</sup>, and NCS<sup>-</sup>. *The Journal of Chemical Physics* **1993**, *98* (2), 800-810.
41. King, B. T.; Michl, J., The Explosive "Inert" Anion CB<sub>11</sub>(CF<sub>3</sub>)<sub>12</sub>. *Journal of the American Chemical Society* **2000**, *122* (41), 10255-10256.
42. Koppel, I. A.; Burk, P.; Koppel, I.; Leito, I.; Sonoda, T.; Mishima, M., Gas-Phase Acidities of Some Neutral Brønsted Superacids: A DFT and ab Initio Study. *Journal of the American Chemical Society* **2000**, *122* (21), 5114-5124.
43. Lipping, L.; Leito, I.; Koppel, I.; Krossing, I.; Himmel, D.; Koppel, I. A., Superacidity of closo-Dodecaborate-Based Brønsted Acids: a DFT Study. *The Journal of Physical Chemistry A* **2015**, *119* (4), 735-743.
44. Lipping, L.; Leito, I.; Koppel, I.; Koppel, I. A., Gas-Phase Brønsted Superacidity of Some Derivatives of Monocarpa-closo-Borates: a Computational Study. *The Journal of Physical Chemistry A* **2009**, *113* (46), 12972-12978.
45. Leito, I. Superacid derivatives in your pocket? [http://ams.ut.ee/wp-content/uploads/2012/03/Superacids\\_Acidity\\_Leito\\_Shanghai\\_2012.pdf](http://ams.ut.ee/wp-content/uploads/2012/03/Superacids_Acidity_Leito_Shanghai_2012.pdf).
46. Mosseri, R.; Sadoc, J. F., Non-crystalline atomic structures: From Glasses to Quasi-Crystals. In *Geometry in Condensed Matter Physics*, WORLD SCIENTIFIC: 1990; Vol. Volume 9, pp 233-283.
47. Blicke, F. F.; Hotelling, E. B., Polycyclic Quaternary Ammonium Salts. I. *Journal of the American Chemical Society* **1954**, *76* (9), 2422-2426.

48. Blicke, F. F.; Hotelling, E. B., Polycyclic Quaternary Ammonium Salts. II. *Journal of the American Chemical Society* **1954**, *76* (9), 2427-2429.
49. Blicke, F. F.; Hotelling, E. B., Polycyclic Quaternary Ammonium Salts. III. *Journal of the American Chemical Society* **1954**, *76* (20), 5099-5103.
50. Ooi, T.; Kameda, M.; Maruoka, K., Design of N-Spiro C2-Symmetric Chiral Quaternary Ammonium Bromides as Novel Chiral Phase-Transfer Catalysts: Synthesis and Application to Practical Asymmetric Synthesis of  $\alpha$ -Amino Acids. *Journal of the American Chemical Society* **2003**, *125* (17), 5139-5151.
51. Olsson, J. S.; Pham, T. H.; Jannasch, P., Poly(N,N-diallylazacycloalkane)s for Anion-Exchange Membranes Functionalized with N-Spirocyclic Quaternary Ammonium Cations. *Macromolecules* **2017**, *50* (7), 2784-2793.
52. Zhou, H.-m.; Sun, W.-j.; Li, J., Preparation of spiro-type quaternary ammonium salt via economical and efficient synthetic route as electrolyte for electric double-layer capacitor. *Journal of Central South University* **2015**, *22* (7), 2435-2439.
53. Ruan, D.; Zuo, F., High Voltage Performance of Spiro-type Quaternary Ammonium Salt Based Electrolytes in Commercial Large Supercapacitors. *Electrochemistry* **2015**, *83* (11), 997-999.
54. Stoychev, G. L.; Auer, A. A.; Neese, F., Automatic Generation of Auxiliary Basis Sets. *Journal of Chemical Theory and Computation* **2017**, *13* (2), 554-562.
55. Cotton, F. A.; Gruhn, N. E.; Gu, J.; Huang, P.; Lichtenberger, D. L.; Murillo, C. A.; Van Dorn, L. O.; Wilkinson, C. C., Closed-shell molecules that ionize more readily than cesium. *Science* **2002**, *298* (5600), 1971-1974.
56. Cotton, F. A.; Donahue, J. P.; Lichtenberger, D. L.; Murillo, C. A.; Villagrán, D., Expedient Access to the Most Easily Ionized Closed-Shell Molecule, W2(hpp)4. *Journal of the American Chemical Society* **2005**, *127* (31), 10808-10809.
57. Yuan, H.; Chang, S.; Bargatin, I.; Wang, N. C.; Riley, D. C.; Wang, H.; Schwede, J. W.; Provine, J.; Pop, E.; Shen, Z.-X.; Pianetta, P. A.; Melosh, N. A.; Howe, R. T., Engineering Ultra-Low Work Function of Graphene. *Nano Letters* **2015**, *15* (10), 6475-6480.
58. Pop, F.; Auban-Senzier, P.; Canadell, E.; Rikken, G. L. J. A.; Avarvari, N., Electrical magnetochiral anisotropy in a bulk chiral molecular conductor. *Nature Communications* **2014**, *5*, 3757.
59. Rikken, G. L. J. A.; Raupach, E.; Krstić, V.; Roth, S., Magnetochiral anisotropy. *Molecular Physics* **2002**, *100* (8), 1155-1160.
60. Schwesinger, R.; Schlemper, H.; Hasenfratz, C.; Willaredt, J.; Dambacher, T.; Breuer, T.; Ottaway, C.; Fletschinger, M.; Boele, J.; Fritz, H.; Putzas, D.; Rotter Heinz, W.; Bordwell Frederick, G.; Satish Amruthur, V.; Ji, G. Z.; Peters, E. M.; Peters, K.; von Schnering Hans, G.; Walz, L., Extremely Strong, Uncharged Auxiliary Bases; Monomeric and Polymer-Supported Polyaminophosphazenes (P2–P5). *Liebigs Annalen* **2006**, *1996* (7), 1055-1081.
61. Koppel, I. A., Limits of Growth in Chemistry of Superacids and Superbases. In *Conference of Centre of Excellence of High Technological Materials for Sustainable Development*, Tartu, 2014.
62. Leito, I.; Koppel Ilmar, A.; Koppel, I.; Kaupmees, K.; Tshepelevitsh, S.; Saame, J., Basicity Limits of Neutral Organic Superbases. *Angewandte Chemie International Edition* **2015**, *54* (32), 9262-9265.
63. Kolomeitsev, A. A.; Koppel, I. A.; Rodima, T.; Barten, J.; Lork, E.; Röschenthaler, G.-V.; Kaljurand, I.; Kütt, A.; Koppel, I.; Mäemets, V.; Leito, I., Guanidinophosphazenes: Design,

Synthesis, and Basicity in THF and in the Gas Phase. *Journal of the American Chemical Society* **2005**, *127* (50), 17656-17666.

64. Kaljurand, I.; Saame, J.; Rodima, T.; Koppel, I.; Koppel, I. A.; Kögel, J. F.; Sundermeyer, J.; Köhn, U.; Coles, M. P.; Leito, I., Experimental Basicities of Phosphazene, Guanidinophosphazene, and Proton Sponge Superbases in the Gas Phase and Solution. *The Journal of Physical Chemistry A* **2016**, *120* (16), 2591-2604.